AGU PUBLICATIONS

Geophysical Research Letters

RESEARCH LETTER
10.1002/2016GL069022

Key Points:
- Global warming precipitation projections are sensitive to convective parameterization
- This sensitivity is distributed nonlinearly across the feasible parameter range
- This can be used to identify key ranges to exclude by observational constraint

Supporting Information:
- Supporting Information S1

Correspondence to:
J. D. Neelin,
neelin@atmos.ucla.edu

Citation:
Bernstein, D. N., and J. D. Neelin (2016), Identifying sensitive ranges in global warming precipitation change dependence on convective parameters, *Geophys. Res. Lett.*, *43*, 5841–5850, doi:10.1002/2016GL069022.

Received 6 APR 2016
Accepted 25 APR 2016
Accepted article online 28 APR 2016
Published online 11 JUN 2016

Identifying sensitive ranges in global warming precipitation change dependence on convective parameters

Diana N. Bernstein[1,2] and J. David Neelin[1]

[1]Department of Atmospheric and Oceanic Sciences, University of California, Los Angeles, Los Angeles, California, USA, [2]Department of Soil and Water Sciences, Robert H. Smith Faculty of Agriculture, Food and Environment, Hebrew University of Jerusalem, Rehovot, Israel

Abstract A branch-run perturbed-physics ensemble in the Community Earth System Model estimates impacts of parameters in the deep convection scheme on current hydroclimate and on end-of-century precipitation change projections under global warming. Regional precipitation change patterns prove highly sensitive to these parameters, especially in the tropics with local changes exceeding 3 mm/d, comparable to the magnitude of the predicted change and to differences in global warming predictions among the Coupled Model Intercomparison Project phase 5 models. This sensitivity is distributed nonlinearly across the feasible parameter range, notably in the low-entrainment range of the parameter for turbulent entrainment in the deep convection scheme. This suggests that a useful target for parameter sensitivity studies is to identify such disproportionately sensitive "dangerous ranges." The low-entrainment range is used to illustrate the reduction in global warming regional precipitation sensitivity that could occur if this dangerous range can be excluded based on evidence from current climate.

1. Introduction

The hydrological cycle poses challenges for climate models, both for present climate and for projections of change under global warming. Biases persist in simulation of current regional climate and variability [*Covey et al.*, 2003; *Sobel et al.*, 2004; *Dai*, 2006; *Zhang and Wang*, 2006; *Stephens et al.*, 2010; *Small et al.*, 2011; *Levine and Turner*, 2012; *Xie et al.*, 2012; *Langenbrunner and Neelin*, 2013; *Neale et al.*, 2013; *Rosa and Collins*, 2013]. Despite some agreement at large spatial scales, there are severe issues with model disagreement on global warming precipitation change at regional and seasonal scales [*Held and Soden*, 2006; *Neelin et al.*, 2006; *Meehl et al.*, 2007; *Solomon et al.*, 2007; *Allan and Soden*, 2008; *Chou et al.*, 2009; *Seager et al.*, 2010; *Tebaldi et al.*, 2011; *Trenberth*, 2011; *Meehl et al.*, 2013], including changes of extremes [*Kharin and Zwiers*, 2005; *Tebaldi et al.*, 2006]. This has contributed to the sense that moist processes—including parameterizations of convection and precipitation and their strong interaction with the large-scale dynamics—remain an underconstrained aspect of climate models. Convective parameterizations can be sensitive to changes in representations of such processes as inclusion of downdrafts or turbulent entrainment [*Derbyshire et al.*, 2004; *Hohenegger and Stevens*, 2013], the latter of which can even affect global climate sensitivity [*Rougier et al.*, 2009; *Sanderson*, 2011; *Sherwood et al.*, 2013]. The differences across a multimodel ensemble, such as Coupled Model Intercomparison Project (CMIP) phases 3 and 5 [*Taylor et al.*, 2012], are often used as an estimate of uncertainty in projections of climate change, despite concerns in that some components are shared across models [*Knutti et al.*, 2010; *Masson and Knutti*, 2011; *Knutti and Sedlacek*, 2013].

While multimodel ensembles have difficulty identifying particular physical processes contributing to the uncertainty, Perturbed Physics Ensembles (PPE), permit systematic examination of sensitivity to parameterized processes. Typically parameters associated with subgrid-scale processes are varied through their feasible range, i.e., the range of values that cannot be excluded a priori [*Allen*, 1999; *Murphy et al.*, 2004; *Jones et al.*, 2005; *Stainforth et al.*, 2005; *Knight et al.*, 2007; *Jackson et al.*, 2008; *Sanderson et al.*, 2008; *Frame et al.*, 2009; *Rougier et al.*, 2009; *Neelin et al.*, 2010; *Collins et al.*, 2011; *Klocke et al.*, 2011; *Sanderson*, 2011; *Brient and Bony*, 2012; *Shiogama et al.*, 2012; *Zhang et al.*, 2012; *Webb et al.*, 2012; *Zamboni et al.*, 2014; *Shiogama et al.*, 2014]. Leading targets for such studies have been errors with respect to climatology in current climate, and the equilibrium climate sensitivity under global warming. A number of these studies indicate that climate sensitivity in their PPE is similar to or greater than climate sensitivity in the multimodel ensembles [*Murphy* *et al*., 2004; *Stainforth et al*., 2005; *Collins et al*., 2011; *Rowlands et al*., 2012; *Yamazaki et al*., 2013] although it is not clear that PPE typically spans the range of the CMIP archive [*Yokohata et al*., 2012, 2013]. Some have sought to reduce error in the model climatology by tuning parameter values or identifying more probable values based on error with respect to observed climatology [*Jones et al*., 2005; *Severijns and Hazeleger*, 2005; *Jackson et al*., 2008; *Zhang et al*., 2012; *Covey et al*., 2013; *Tett et al*., 2013].

In this study, parameter sensitivity in the fully coupled Community Earth System Model (CESM1) is examined for global warming projection runs, as well as historical climate, specifically for key parameters in the deep convection scheme. Insufficiently constrained parameters affecting deep convection are known to affect simulation of current climate and global average climate sensitivity [e.g., *Neale et al*., 2008; *Sanderson*, 2011; *Covey et al*., 2013; *Guo et al*., 2015; *Qian et al*., 2015] and are hypothesized here to contribute strongly to sensitivity in projections of regional precipitation change.

Leading order factors to be determined for parameter sensitivity are the magnitude and spatial distribution of the sensitivity across the feasible range for each parameter, and for parameters exhibiting strong sensitivity, the degree of nonlinearity within that parameter domain. Here both are assessed using runs along parameter axes, since this involves a number of simulations of order N, where N is the number parameters, and because it is most straightforward to interpret in terms of the physical processes. Given that substantial sensitivity and nonlinearity is found, future work can leverage results here to estimate nonlinear interactions among parameters. Nonlinearity of parameter dependence is a crucial factor that can affect many aspects of the climate sensitivity problem, especially for variables such as precipitation. Sparse parameter-space sampling in PPE and use of multimodel ensemble averages each contain implicit assumptions of weak nonlinearity. Severe cases of rapidly varying parameter dependence have been noted in intermediate complexity models [*Chekroun et al*., 2014] but smoothly nonlinear dependence in important metrics occur in at least one climate model [*Neelin et al*., 2010; *Bracco et al*., 2013]. In addition to assessing the degree of nonlinearity here, a focus will be on whether this is can identify sensitive parameter ranges in which observational constraints from current climate could reduce the uncertainty range in projections of future climate. If so, the order N process used here can be an efficient screening process for identifying leading opportunities for uncertainty reduction.

2. Setup

The set of experiments is done as branch runs starting from particular years of an existing standard parameter simulation with the Community Climate System Model 4 (CCSM4; i.e., a subset of CESM1) with historical and Representative Concentration Pathway 8.5 (RCP8.5) radiative forcing [*Meinshausen et al*., 2011]. An ensemble of 15 CESM1 standard parameter simulations serves as a control over the periods 1976–2005 for the historical and 2071–2100 for the RCP8.5 end-of-century simulations. Values of four parameters are varied relative to the control: the deep convective adjustment time, τ; the deep convective entrainment parameter, dmpdz; the deep convective downdraft mass flux fraction, α; and the deep convective evaporation efficiency, k_e, in the deep convective scheme [*Zhang and McFarlane*, 1995], which includes turbulent mixing between the parcel and the environment by *Neale et al*. [2008]. The branch-run methodology helps to reduce the computational burden of several hundred years spin-up plus historical and RCP8.5 simulation that would potentially be required at each parameter value, if each followed the full equilibration protocol of CMIP5 simulations. This takes advantage of the focus on evaluation of hydrological cycle projected changes which tend to adjust more quickly than aspects of the climate system involving the deep ocean. Climate drift associated with parameter changes may occur [e.g., *Collins et al*., 2011; *Shiogama et al*., 2012], although for many parameters this can be modest [e.g., *Irvine et al*., 2013], so it is necessary to quantify equilibration for key metrics of interest. The equilibration process for global warming precipitation change for the parameter exhibiting largest changes occurs substantially within the first decade and exhibits little drift in the last 20 years, as documented in Figure S1 in the supporting information (along with further details on experimental design). This would not necessarily apply for variables more strongly dependent on subsurface ocean equilibration.

3. Sensitivity of Climatology Simulation in the Historical Period

As background for the examination of global warming precipitation change sensitivity, Figure 1 shows an example of the parameter sensitivity under current climate for the coupled system in the historical run for

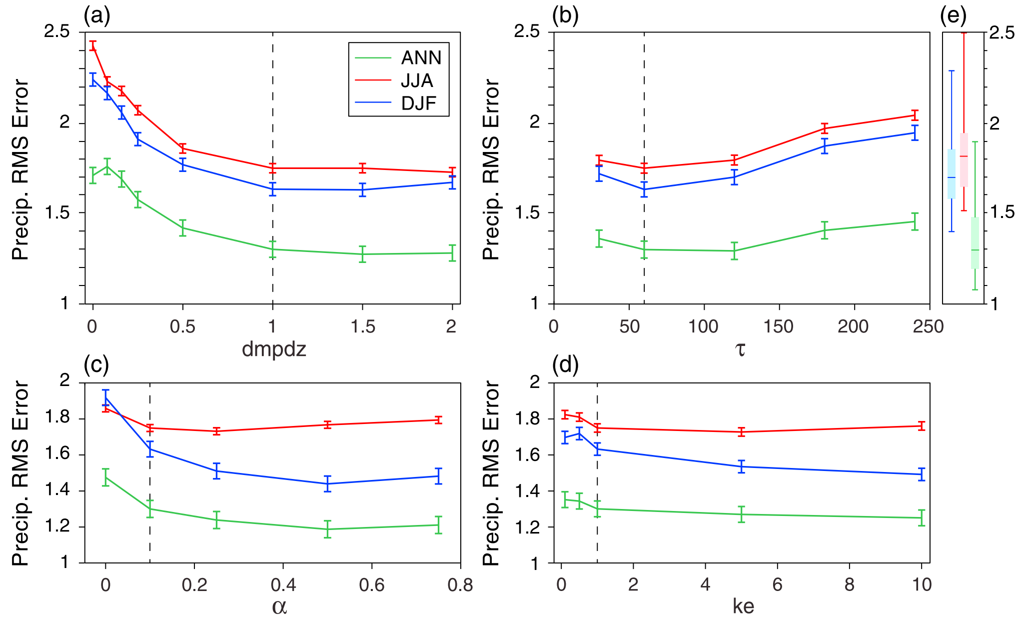

Figure 1. Parameter dependence in CESM1 for historical runs of the coupled climate model (1986–2005). RMSE of precipitation for DJF, JJA, and annual average climatologies, respectively (with respect to GPCP, in mm/d) as a function of (a) the deep convective entrainment parameter dmpdz (10^{-3} m^{-1}); (b) the deep convective timescale parameter τ (minutes); (c) downdraft fraction α; (d) evaporation efficiency k_e (10^{-6}(kg m^{-2} s^{-1})$^{-1/2}$ s^{-1}). The vertical line on each parameter axis indicates standard case values. (e) RMSE range (whiskers) and 25th–75th percentiles (bars) from the CMIP5 ensemble for the same time period.

December–February (DJF) and June–August (JJA) precipitation as a function of four parameters. The area-weighted root-mean-square error (RMSE) relative to Global Precipitation Climatology Project (GPCP) [*Adler et al.*, 2003] v2.2 observed precipitation climatology is shown, and over most of the range, the evolution is relatively smooth (see supporting information for error bar computation). The CESM1 parameter dependence as a function of entrainment illustrates an effect that may be important for both individual model assessment and multimodel exploration. The sensitivity and nonlinearity of the parameter dependence are high in the low-entrainment range. Indeed, the sensitivity of precipitation error to the range of entrainment (Figure 1a) between zero and values approaching 1 km^{-1} is sufficiently strong (30–40% relative to the minimum RMSE) to flag this as a range needing careful attention due to the strong sensitivity and likely nonlinearity. Smaller-amplitude echoes of this behavior may be seen in other variables, although the difference between maximum and minimum RMSE is typically around 15% (range from 5% for JJA k_e to 30% for DJF α). The RMSE range and 25th–75th percentiles from an ensemble of 36 CMIP5 models (Figure 1e) indicate that a criterion of lying within the range of these models in this RMSE metric would not exclude any portion of the parameter ranges. A single RMSE metric is of course an incomplete assessment of the historical simulation (and there are often trade-offs among metrics, e.g., *Neelin et al.* [2010]). The question here is whether coordination with evaluation of sensitivity under global warming might highlight parameter ranges most in need of additional constraint.

4. Sensitivity of Projected Changes Under Global Warming

Figure 2a shows the projected change in the precipitation climatology for JJA for 2081–2100 relative to the 1986–2005 base period under the RCP8.5 scenario for CESM1 standard parameters. It is highly consistent with the CCSM4 precipitation change pattern in the 1° resolution version in the CMIP5 archive. CESM shows strong positive precipitation trend in the equatorial Indian Ocean for DJF and in the Pacific ITCZ and southeastern Asia for JJA. A negative precipitation trend is projected as expected over much of the Subtropics but organized with intense reductions in certain regions, typically along the margins of the convection zones where precipitation has shifted.

Figures 2b–2e shows examples of the sensitivity of projected precipitation change under RCP8.5, for JJA as a function of four parameters. The sensitivity is illustrated as the difference across a feasible range for each

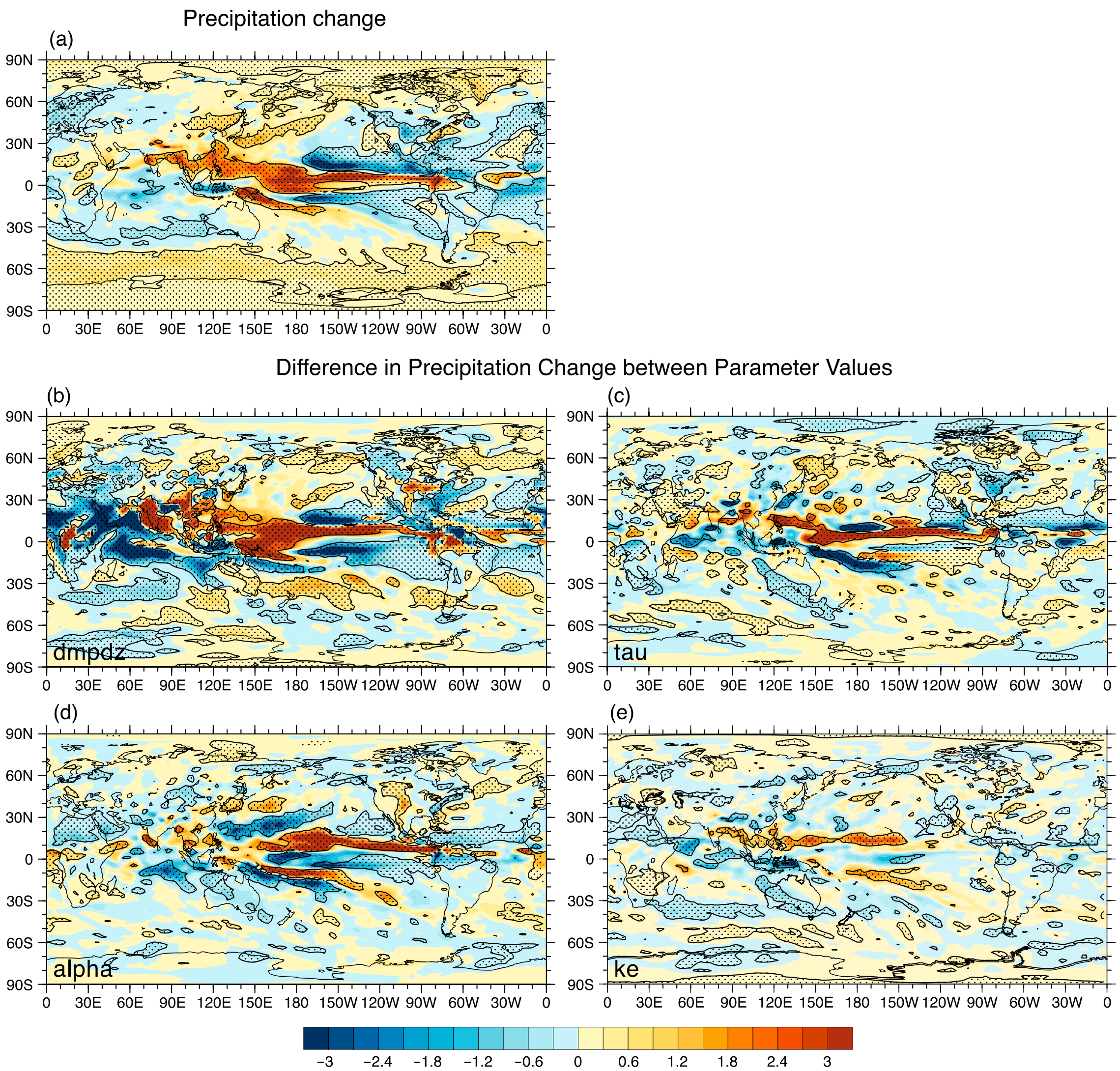

Figure 2. (a) Precipitation (mm/d) change for 2081–2100 relative to the 1986–2005 base period under the RCP8.5 global warming scenario for CESM1 standard values for JJA. Differences in projected JJA precipitation change (mm/d) under global warming (2081–2100 relative to the 1986–2005 base period) for simulations done with different parameter values. Differences are across the feasible range for each parameter: (b) entrainment (case at 2×10^{-3} m^{-1} minus case at 0 m^{-1}); (c) deep convective adjustment time (240 min case minus 30 min case); (d) downdraft fraction (0.75 case minus case at 0); (e) evaporation efficiency (10^{-7}(kg m^{-2} s^{-1})$^{-1/2}$ s^{-1} case minus 10^{-5}(kg m^{-2} s^{-1})$^{-1/2}$ s^{-1} case). Stippled areas pass a *t* test at the 95% level.

parameter. In other words the precipitation change for 2081–2100 relative to the 1986–2005 base period is calculated for the lowest value of the parameter and again for simulations with the highest value of the parameter and then the *difference* between these two projections is presented in the figures. The ideal case would be if the amplitudes of these differences between projected changes would be much smaller than the projected change itself. Unfortunately this is far from being the case. For each of the parameter perturbations across the respective feasible range, differences in the end of century projections for global warming precipitation change regionally exceed 3 mm/d. The typical amplitude of difference in projected change in precipitation across the feasible parameter range is thus as large as the signal that climate models seek to predict.

These differences in precipitation projection across parameter ranges are comparable to differences among CMIP5 model precipitation projections (see, e.g., *Collins et al*. [2013] and supporting information Figure S2). This suggests that differences in projected precipitation change obtained by parameter perturbation in a single model in Figures 2b–2e can serve to a substantial extent as a prototype for the differences encountered among different models. If poorly constrained parameter ranges within a single model can yield such differences, then it is not surprising that an ensemble of models that have undergone different development

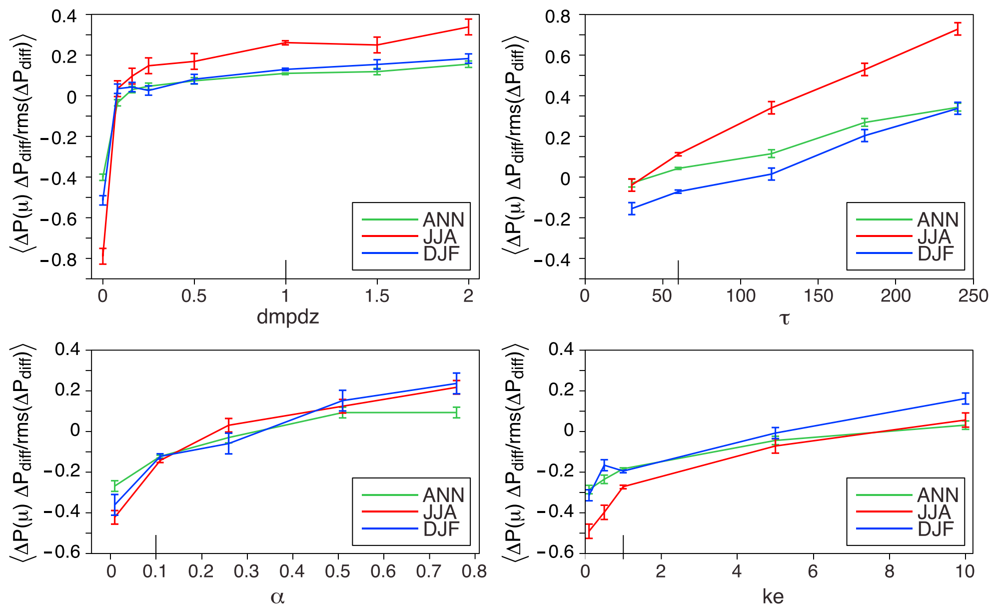

Figure 3. Spatial-projection measure of parameter sensitivity for JJA, DJF, and annual average global warming precipitation change ΔP (difference of the 2081–2100 average relative to 1986–2005): ΔP at each value of the parameter, projected on the spatial pattern of the sensitivity across the whole range (units mm/d; *y* axis scaling is the same for each panel): (a) entrainment ($10^{-3}\,\mathrm{m}^{-1}$), (b) convective timescale (minutes), (c) downdraft fraction, and (d) evaporation efficiency ($10^{-6}(\mathrm{kg\,m}^{-2}\,\mathrm{s}^{-1})^{-1/2}\,\mathrm{s}^{-1}$).

choices for a similar set of physical processes should yield differences in projected precipitation patterns. An advantage of the perturbed physics ensemble, relative to a multimodel ensemble, is that here the physical process responsible for each sensitivity pattern is known. Furthermore, the sensitivity of different portions of the parameter range can be assessed and the implications of each portion of the parameter range for quantities that can be constrained against observations in current climate can be examined.

These leading effects in the hydrological change as a function of parameter tend to occur on time scales that are relatively short compared to deep ocean equilibration. For the examples shown in Figure 2, the strong, statistically significant signal due to the parameter dependence is established with only modest differences in global average temperature change and only modest differences in the base period global average temperature difference.

5. An Example of a Dangerous Range and Potential for Uncertainty Reduction

The sensitivity seen across the feasible ranges in Figures 2b–2d is not necessarily evenly distributed as a function of parameter. There are indications from other model systems that the parameter dependence can be smooth but with substantial nonlinearity, e.g., a large quadratic component, for metrics of climatology and global warming change [*Neelin et al.*, 2010; *Sanderson*, 2011; *Bracco et al.*, 2013; *Zamboni et al.*, 2014]. In the case of global warming change, a different measure of sensitivity must be used than the RMSE relative to observations shown for climatology (Figure 1). Using RMSE relative to the standard case would privilege one particular parameter setting.

Here we propose a measure that does not assume a form of the nonlinearity and does not privilege the standard case: the projection of the precipitation change $\Delta P(\mu)$ with respect to each parameter μ, onto the spatial pattern for the sensitivity identified by the difference across the feasible range ΔP_{diff}. This is given by: $\langle \Delta P(\mu)\Delta P_{\mathrm{diff}}\rangle/\mathrm{RMS}(\Delta P_{\mathrm{diff}})$, where $\Delta P_{\mathrm{diff}} = \Delta P(\mu_{\mathrm{max}}) - \Delta P(\mu_{\mathrm{min}})$, $\langle\,\rangle$ denotes area-weighted spatial averaging, and RMS( ) denotes the spatial root-mean-square across the region of interest, here global. The difference in this measure across the feasible range yields $\mathrm{RMS}(\Delta P_{\mathrm{diff}})$, while the parameter dependence of the measure shows how this spatial pattern of sensitivity is distributed across the range. Figure 3 shows this measure for each parameter (see supporting information for error bar computation). Strong nonlinearity is seen for entrainment, with high sensitivity in the low-entrainment range. In contrast, the convective timescale has a relatively

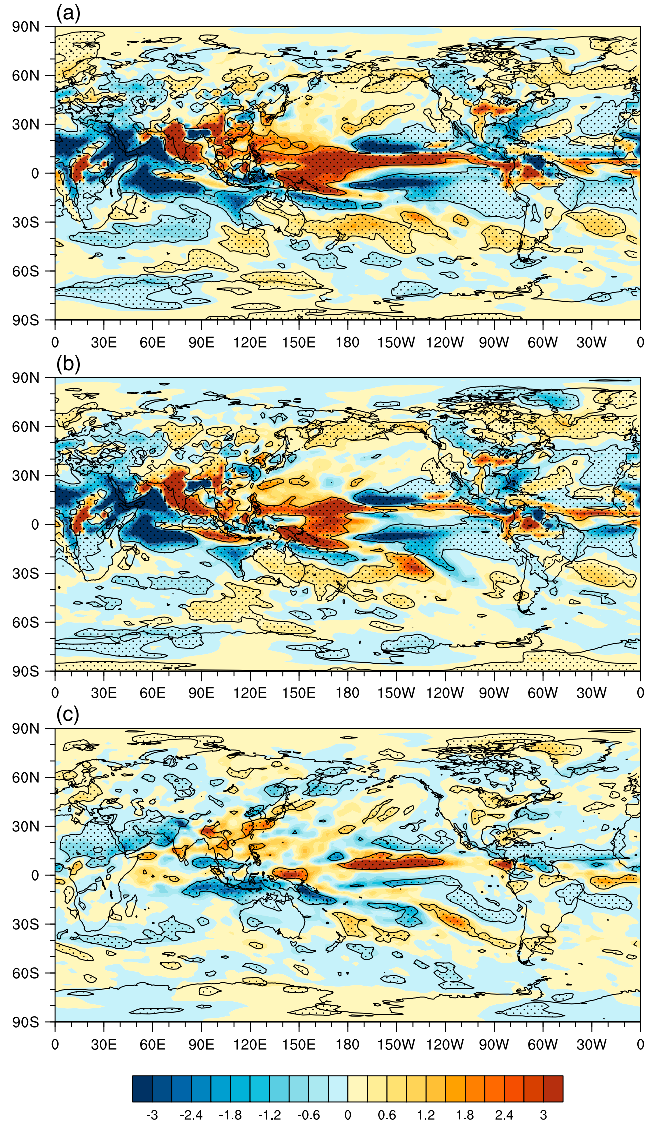

Figure 4. Sensitivity of projected precipitation change (mm/d) for JJA under RCP8.5 (2081–2100 to 1986–2005), but as measured by (a) the difference across the entire feasible range, between entrainment parameter case dmpdz = 2×10^{-3} m^{-1} minus the case at dmpdz = 0; (b) as in Figure 4a but just across the dangerous range, dmpdz = 0.5×10^{-3} m^{-1} minus the case at dmpdz = 0; (c) as in Figure 4a but for a reduced range, dmpdz = 2×10^{-3} m^{-1} minus the case at dmpdz = 0.5×10^{-3} m^{-1}, i.e., excluding the dangerous range. Stippled areas pass a *t* test at the 95% level.

linear parameter dependence, since sensitivity across the full range is comparable in magnitude. Downdraft fraction and evaporation efficiency exhibit intermediate degrees of nonlinearity. Ranges in which a disproportionate share of the sensitivity arises deserve special scrutiny. As a shorthand, we use the term "dangerous ranges" for such strongly sensitive, nonlinear parameter ranges.

Although the spatial projection metric in Figure 3 captures leading behavior, it is not a full measure of the nonlinearity in spatial pattern. Figure 4 thus shows spatial patterns for the sensitivity of precipitation change across portions of the parameter range in entrainment discussed above. Figure 4a shows the difference across the full range for reference (as in Figure 2b). Figure 4b shows the difference in ΔP across the dangerous, low-entrainment range, while Figure 4c shows the difference in projections of ΔP across the entire remainder of the range. The difference across the dangerous range in Figure 4b is almost comparable to the difference across the full range. Figure 4c shows how dramatically the uncertainty associated with this parameter could be reduced if constraints based on consistency with observations in the historical period can eliminate the low-entrainment range. This points to a large potential for uncertainty reduction.

The entrainment example in Figures 3b and 4 illustrates another important factor: that in at least some cases a range with strong sensitivity for global warming hydrological cycle change can correspond to a sensitive, nonlinear range for hydrological cycle variables in the current climate, as seen in Figure 1a. This was also found in a parameter affecting the onset of deep convection in the International Center for Theoretical Physics model [*Neelin et al*., 2010; *Bracco et al*., 2013]. When this occurs, constraints from the current climate can potentially be brought to bear. Figure 1a shows that error in the climatological precipitation field relative to observations is one metric that suggests that the low-entrainment range is less consistent with observations in the current climate. Earlier versions of the CESM atmospheric component (Community Atmosphere Model version 3) [*Collins et al*., 2006], which was included in CMIP3, used nonentraining deep convection, so the low-entrainment range has been considered plausible and cannot be dismissed a priori. However, work on statistics for the relationship of the onset of deep convection to free tropospheric moisture and temperature provides mounting evidence that use of the low value of entrainment is inconsistent with observations [*Holloway and Neelin*, 2009; *Jensen and Del Genio*, 2006; *Sahany et al*., 2012]. This includes assessment of convective onset against observations in versions of CESM [*Sahany et al*., 2012, 2014] that weigh strongly against the low-entrainment range. These fast-process diagnostics at the timescale of the parameterized process complement metrics from the climatology, such as seen in Figure 1a. The entrainment parameter thus provides an example where parameter perturbation identifies a range that, if eliminated, results in substantial reduction in the contribution of that parameter to the uncertainty of projected precipitation change, highlighting the usefulness of such observational efforts to further constrain this range.

6. Discussion and Conclusions

To understand and constrain the uncertainty for global warming hydrological cycle quantities, it is useful to assess uncertainties associated with each model parameter. Here we use a branch-run methodology in CESM1 to provide an estimate of this that is directly associated with the historical and a commonly evaluated global warming projection scenario, RCP8.5. Short 30 year runs, of which 20 years are evaluated here to permit 10 years of equilibration, give sufficient statistical significance on precipitation climatology to evaluate parameter sensitivities where they are large in the sense of being a substantial fraction of the signal being predicted.

In the historical period, precipitation patterns exhibit considerable sensitivity to each parameter, with local changes exceeding 3 mm/d. However, in terms of RMSE relative to the GPCP observational estimate, individual parameters can contribute to increases or decreases in the RMSE within their individual ranges typically on the order of 15% which would not necessarily exclude versions of the model with any of the parameter settings from being included in a model ensemble such as CMIP5. Indications of nonlinearity in the parameter dependence may nonetheless be noted within the historical period.

The key focus here is on the parameter dependence of the end of century projections for global warming precipitation change for the coupled model. Across the feasible range for each parameter, differences in the projected global warming precipitation change have values comparable to the projected change itself. Regional differences in the projected precipitation change, especially in the tropics, exceed 3 mm/d, which is comparable to differences in global warming predictions among the CMIP5 models. While PPE do not sample structural differences in parameterizations as would occur in an ensemble of different models, and it is highly possible that parameter perturbations in other parts of the physics could contribute comparably. It is clear that uncertainties in the deep convective parameters contribute substantially to the uncertainty in projections of future precipitation change in this model.

Within the feasible range for certain parameters, this sensitivity can be distributed nonlinearly. In particular, differences across the low-entrainment range for the deep convective scheme are disproportionately larger than changes across the remainder of the feasible range. As a metric of this, we compute a projection of the global warming precipitation change at each parameter value onto the spatial pattern of this change evaluated across the entire feasible range. In other words, we choose a single key spatial pattern important to the uncertainty for each parameter and ask how the contributions of this are distributed as a function of parameter. Parameter ranges that exhibit strong sensitivity relative to the a priori constraints that set the feasible range can contribute disproportionately to uncertainty, and thus termed dangerous ranges. The low-entrainment range in this model provides an example of such a dangerous range. The uncertainty associated with this parameter can be substantially reduced (by roughly 80% across one eighth of the feasible range) if this dangerous range can be excluded. Evidence from the RMSE with respect to current precipitation climatology evaluated here, and constraints from fast-process diagnostics for the onset of convection [e.g., *Sahany et al*., 2012, 2014] suggest that this low-entrainment range should indeed be excluded. For the other parameters presented here, one was sensitive but with a relatively linear distribution across the feasible range, and two exhibited substantial nonlinearity, although less drastic than that seen in entrainment. As a rule of thumb, 40% of the uncertainty across a small fraction of the feasible range (e.g., less than one quarter, which would imply double the slope within the dangerous range than within the remainder) would be a reasonable criterion to flag a range for special scrutiny. Because the global warming precipitation change appears to be particularly sensitive to parameter perturbation, we argue that it is worthwhile to standardly estimate this at the same time as evaluating parameter-dependent behavior in current climatology.

Identification of such dangerous ranges, where they exist, in multiple parameters and potentially in multiple models can help to pinpoint the behavior ranges of physical processes that should be priorities for additional observational constraint. The indications are that multiple parameters can contribute to hydrological cycle sensitivity. While narrowing the overall spread in a multimodel ensemble should be expected to be a gradual process, the dangerous ranges potentially represent the low-hanging fruit.

Acknowledgments
This work was supported in part by National Science Foundation (NSF) AGS-1102838/AGS-1540518, Department of Energy DE-SC0006739, and National Oceanic and Atmospheric Administration NA14OAR4310274, with high-performance computing support from Yellowstone (ark:/85065/d7wd3xhc) provided by NCAR's Computational and Information Systems Laboratory, sponsored by NSF. CESM output data used in this study are available from the authors (dianab@atmos.ucla.edu) following guidelines in the CESM data plan (www.cesm.ucar.edu/management/docs/data.mgt.plan.2011.pdf). The GPCP combined precipitation data were developed and computed by the NASA/Goddard Space Flight Center's Laboratory for Atmospheres and provided by NOAA/OAR/ESRL PSD, Boulder, Colorado, USA, at http://www.esrl.noaa.gov/psd/. The authors thank S. Sahany and B. Langenbrunner for discussions and J.E. Meyerson for graphical assistance.

References

Adler, R. F., et al. (2003), The version 2 Global Precipitation Climatology Project (GPCP) monthly precipitation analysis (1979–present), *J. Hydrometeorol.*, *4*, 1147–1167.

Allan, R. P., and B. J. Soden (2008), Atmospheric warming and the amplification of precipitation extremes, *Science*, *321*, 1481–1484.

Allen, M. (1999), Do-it-yourself climate prediction, *Nature*, *401*, 642–642.

Bracco, A., J. D. Neelin, H. Luo, J. C. McWilliams, and J. E. Meyerson (2013), High-dimensional decision dilemmas in climate models, *Geosci. Model Dev.*, *6*, 1673–1687, doi:10.5194/gmd-6-1673-2013.

Brient, F., and S. Bony (2012), How may low-cloud radiative properties simulated in the current climate influence low-cloud feedbacks under global warming?, *Geophys. Res. Lett.*, *39*, L20807, doi:10.1029/2012GL053265.

Chekroun, M. D., J. D. Neelin, D. Kondrashov, J. C. McWilliams, and M. Ghil (2014), Rough parameter dependence in climate models and the role of Ruelle-Pollicott resonances, *Proc. Natl. Acad. Sci. U.S.A.*, *111*(5), 1684–1690, doi:10.1073/pnas.1321816111.

Chou, C., J. D. Neelin, C.-A. Chen, and J.-Y. Tu (2009), Evaluating the "rich-get-richer" mechanism in tropical precipitation change under global warming, *J. Clim.*, *22*, 1982–2005, doi:10.1175/2008JCLI2471.1.

Collins, M., B. B. B. Booth, B. Bhaskaran, G. R. Harris, J. M. Murphy, D. M. H. Sexton, and M. J. Webb (2011), Climate model errors, feedbacks and forcings: A comparison of perturbed physics and multi-model ensembles, *Clim. Dyn.*, *36*, 1737–1766.

Collins, M., et al. (2013), Long-term climate change: Projections, commitments and irreversibility, in: *Climate Change 2013: The Physical Science Basis. Contribution of Working Group I to the Fifth Assessment Report of the Intergovernmental Panel on Climate Change*, edited by T. F. Stocker et al., Cambridge Univ. Press, Cambridge, U. K., and New York.

Collins, W. D., P. J. Rasch, B. A. Boville, J. J. Hack, J. R. McCaa, D. L. Williamson, B. P. Briegleb, C. M. Bitz, S. J. Lin, and M. H. Zhang (2006), The formulation and atmospheric simulation of the Community Atmosphere Model version 3 (CAM3), *J. Clim.*, *19*, 2144–2161, doi:10.1175/JCLI3760.1.

Covey, C., K. M. AchutaRao, U. Cubasch, P. Jones, S. J. Lambert, M. E. Mann, T. J. Phillips, and K. E. Taylor (2003), An overview of results from the Coupled Model Intercomparison Project, *Global Planet. Change*, *37*, 103–133.

Covey, C., D. D. Lucas, J. Tannahill, X. Garaizar, and R. Klein (2013), Efficient screening of climate model sensitivity to a large number of perturbed input parameters, *J. Adv. Model. Earth Syst.*, *5*, 598–610, doi:10.1002/jame.20040.

Dai, A. (2006), Precipitation characteristics in eighteen coupled climate models, *J. Clim.*, *19*, 4605–4630.

Derbyshire, S. H., I. Beau, P. Bechtold, J.-Y. Grandpeix, J.-M. Piriou, J.-L. Redelsperger, and P. M. M. Soares (2004), Sensitivity of moist convection to environmental humidity, *Q. J. R. Meteorol. Soc.*, *130*, 3055–3079.

Frame, D. J., T. Aina, C. M. Christensen, N. E. Fall, S. H. E. Knight, C. Piani, S. M. Rosier, K. Yamazaki, Y. Yamazaki, and M. R. Allen (2009), The climateprediction.net BBC climate change experiment: Design of the coupled model ensemble, *Philos. Trans. R. Soc., London A*, *367*, 855–870, doi:10.1098/rsta.2008.0240.

Guo, Z., M. Wang, Y. Qian, V. E. Larson, S. Ghan, M. Ovchinnikov, P. A. Bogenschutz, A. Gettelman, and T. Zhou (2015), Parametric behaviors of CLUBB in simulations of low clouds in the Community Atmosphere Model (CAM), *J. Adv. Model. Earth Syst.*, *7*, 1005–1025, doi:10.1002/2014MS000405.

Held, I. M., and B. J. Soden (2006), Robust responses of the hydrological cycle to global warming, *J. Clim.*, *19*, 5686–5699.

Hohenegger, C., and B. Stevens (2013), Preconditioning deep convection with cumulus congestus, *J. Atmos. Sci.*, *70*, 448–464, doi:10.1175/JAS-D-12-089.1.

Holloway, C. E., and J. D. Neelin (2009), Moisture vertical structure, column water vapor, and tropical deep convection, *J. Atmos. Sci.*, *66*, 1665–1683, doi:10.1175/2008JAS2806.1.

Irvine, P. J., L. J. Gregoire, D. J. Lunt, and P. J. Valdes (2013), An efficient method to generate a perturbed parameter ensemble of a fully coupled AOGCM without flux-adjustment, *Geosci. Model Dev.*, *6*, 1447–1462, doi:10.5194/gmd-6-1447-2013.

Jackson, C., M. Sen, G. Huerta, Y. Deng, and K. Bowman (2008), Error reduction and convergence in climate prediction, *J. Clim.*, *21*, 6698–6709.

Jensen, M. P., and A. D. Del Genio (2006), Factors limiting convective cloud-top height at the ARM Nauru Island climate research facility, *J. Clim.*, *19*, 2105–2117, doi:10.1175/JCLI3722.1.

Jones, C., J. Gregory, R. Thorpe, P. Cox, J. Murphy, D. Sexton, and P. Valdes (2005), Systematic optimization and climate simulation of FAMOUS, a fast version of HadCM3, *Clim. Dyn.*, *25*, 189–204, doi:10.1007/s00382-007-0325-y.

Kharin, V. V., and F. W. Zwiers (2005), Estimating extremes in transient climate change simulations, *J. Clim.*, *18*, 1156–1173.

Klocke, D., R. Pincus, and J. Quaas (2011), On constraining estimates of climate sensitivity with present-day observations through model weighting, *J. Clim.*, *24*, 6092–6099.

Knight, C. G., et al. (2007), Association of parameter, software, and hardware variation with large-scale behavior across 57,000 climate models, *Proc. Natl. Acad. Sci. U.S.A.*, *104*, 12,259–12,264, doi:10.1175/JCLI3430.1.

Knutti, R., and J. Sedlacek (2013), Robustness and uncertainties in the new CMIP5 climate model projections, *Nat. Clim. Change*, *3*, 369–373.

Knutti, R., R. Furrer, C. Tebaldi, J. Cermak, and G. A. Meehl (2010), Challenges in combining projections from multiple climate models, *J. Clim.*, *23*, 2739–2758.

Langenbrunner, B., and J. D. Neelin (2013), Analyzing ENSO teleconnections in CMIP models as a measure of model fidelity in simulating precipitation, *J. Clim.*, *26*, 4431–4446, doi:10.1175/JCLI-D-12-00542.1.

Levine, R. C., and A. G. Turner (2012), Dependence of Indian monsoon rainfall on moisture fluxes across the Arabian Sea and the impact of coupled model sea surface temperature biases, *Clim. Dyn.*, *38*, 2167–2190.

Masson, D., and R. Knutti (2011), Climate model genealogy, *Geophys. Res. Lett.*, *38*, L08703, doi:10.1029/2011GL046864.

Meehl, G. A., W. M. Washington, J. M. Arblaster, A. H. Haiyan Teng, J. E. Kay, A. Gettelman, D. M. Lawrence, B. M. Sanderson, and W. G. Strand (2013), Climate change projections in CESM1 (CAM5) compared to CCSM4, *J. Clim.*, *26*, 6287–6308.

Meehl, G., et al. (2007), Global climate projections, in: *Climate Change 2007: The Physical Science Basis. Contribution of Working Group I to the Fourth Assessment Report of the Intergovernmental Panel on Climate Change*, edited by S. Solomon, D. Qin, and M. Manning, p. 996, Cambridge Univ. Press, Cambridge and New York.

Meinshausen, M., et al. (2011), The RCP greenhouse gas concentrations and their extension from 1765 to 2300, *Clim. Change*, *109*, 213–241, doi:10.1007/s10584-011-0156-z.

Murphy, J. M., D. M. H. Sexton, D. N. Barnett, G. S. Jones, M. J. Webb, M. Collins, and D. A. Stainforth (2004), Quantification of modelling uncertainties in a large ensemble of climate change simulations, *Nature*, *430*, 768–772.

Neale, R. B., J. J. Richter, and M. Jochum (2008), The impact of convection on ENSO: From a delayed oscillator to a series of events, *J. Clim.*, *21*, 5904–5924, doi:10.1175/2008JCLI2244.1.

Neale, R., J. Richter, S. Park, P. H. Lauritzen, S. J. Vavrus, P. J. Rasch, and M. Zhang (2013), The mean climate of the Community Atmosphere Model (CAM4) in forced SST and fully coupled experiments, *J. Clim.*, *26*, 5150–5168, doi:10.1175/JCLI-D-12-00236.1.

Neelin, J. D., M. Munnich, H. Su, J. E. Meyerson, and C. E. Holloway (2006), Tropical drying trends in global warming models and observations, *Proc. Natl. Acad. Sci. U.S.A.*, *103*, 6110–6115.

Neelin, J. D., A. Bracco, H. Luo, J. C. McWilliams, and J. E. Meyerson (2010), Considerations for parameter optimization and sensitivity in climate models, *Proc. Natl. Acad. Sci. U.S.A.*, *107*, 21,349–21,354, doi:10.1073/pnas.1015473107.

Qian, Y., et al. (2015), *Parametric* sensitivity analysis of precipitation at global and local scales in the Community Atmosphere Model CAM5, *J. Adv. Model. Earth Syst.*, *7*, 382–411, doi:10.1002/2014MS000354.

Rosa, D., and W. D. Collins (2013), A case study of subdaily simulated and observed continental convective precipitation: CMIP5 and multiscale global climate models comparison, *Geophys. Res. Lett.*, *40*, 5999–6003, doi:10.1002/2013GL057987.

Rougier, J., D. M. H. Sexton, J. M. Murphy, and D. Stainforth (2009), Analyzing the climate sensitivity of the HadSM3 climate model using ensembles from different but related experiments, *J. Clim.*, *22*, 3540–3557, doi:10.1175/2008JCLI2533.1.

Rowlands, D. J., et al. (2012), Broad range of 2050 warming from an observationally constrained large climate model ensemble, *Nat. Geosci.*, *5*, 256–260.

Sahany, S., J. D. Neelin, K. Hales, and R. Neale (2012), Temperature-moisture dependence of the deep convective transition as a constraint on entrainment in climate models, *J. Atmos. Sci.*, *69*, 1340–1358, doi:10.1175/JAS-D-11-0164.1.

Sahany, S., J. D. Neelin, K. Hales, and R. B. Neale (2014), Deep convective transition characteristics in the NCAR CCSM and changes under global warming, *J. Clim.*, *27*, 9214–9232, doi:10.1175/JCLI-D-13-00747.1.

Sanderson, B. M. (2011), A multimodel study of parametric uncertainty in predictions of climate response to rising greenhouse gas concentrations, *J. Clim.*, *24*, 1362–1377, doi:10.1175/2010JCLI3498.1.

Sanderson, B. M., C. Piani, W. J. Ingram, D. A. Stone, and M. R. Allen (2008), Towards constraining climate sensitivity by linear analysis of feedback patterns in thousands of perturbed-physics GCM simulations, *Clim. Dyn.*, *30*, 175–190.

Seager, R., N. Naik, and G. A. Vecchi (2010), Thermodynamic and dynamic mechanisms for large-scale changes in the hydrological cycle in response to global warming, *J. Clim.*, *23*, 4651–4668.

Severijns, C. A., and W. Hazeleger (2005), Optimizing parameters in an atmospheric general circulation model, *J. Clim.*, *18*, 3527–3535, doi:10.1175/JCLI3430.1.

Sherwood, S. C., S. Bony, and J.-L. Dufresne (2013), Spread in model climate sensitivity traced to atmospheric convective mixing, *Nature*, *505*, 37–42, doi:10.1038/nature12829.

Shiogama, H., et al. (2012), Perturbed physics ensemble using the MIROC5 coupled atmosphere ocean GCM without flux corrections: Experimental design and results, *Clim. Dyn.*, *39*, 3041–3056.

Shiogama, H., M. Watanabe, T. Ogura, T. Yokohata, and M. Kimoto (2014), Multi-parameter multi-physics ensemble (MPMPE): A new approach exploring the uncertainties of climate sensitivity, *Atmos. Sci. Lett.*, *15*, 97–102, doi:10.1002/asl2.472.

Small, R., S.-P. Xie, E. Maloney, S. Szoeke, and T. Miyama (2011), Intraseasonal variability in the fareast Pacific: Investigation of the role of air-sea coupling in a regional coupled model, *Clim. Dyn.*, *36*, 867–890.

Sobel, A. H., S. E. Yuter, C. S. Bretherton, and G. N. Kiladis (2004), Large-scale meteorology and deep convection during TRMM KWAJEX, *Mon. Weather Rev.*, *132*, 422–444.

Solomon, S., D. Qin, M. Manning, Z. Chen, M. Marquis, K. B. Averyt, M. Tignor, and H. L. Miller (2007), *Intergovernmental Panel on Climate Change: Contribution of Working Group I to the Fourth Assessment Report of the Intergovernmental Panel on Climate Change (2007) The Physical Science Basis*, Cambridge Univ. Press, Cambridge, U. K.

Stainforth, D. A., et al. (2005), Uncertainty in predictions of climate response to rising levels or greenhouse gases, *Nature*, *433*, 403–406, doi:10.1175/JCLI3430.1.

Stephens, G. L., T. L'Ecuyer, R. Forbes, A. Gettlemen, J.-C. Golaz, A. Bodas-Salcedo, K. Suzuki, P. Gabriel, and J. Haynes (2010), Dreary state of precipitation in global models, *J. Geophys. Res.*, *115*, D24211, doi:10.1029/2010JD014532.

Taylor, K. E., R. J. Stouffer, and G. A. Meehl (2012), An overview of CMIP5 and the experiment design, *Bull. Am. Meteorol. Soc.*, *93*, 485–498.

Tebaldi, C., K. Hayhoe, J. M. Arblaster, and G. A. Meehl (2006), Going to the extremes: An intercomparison of model-simulated historical and future changes in extreme events, *Clim. Change*, *79*, 185–211.

Tebaldi, C., J. M. Arblaster, and R. Knutti (2011), Mapping model agreement on future climate projections, *Geophys. Res. Lett.*, *38*, L23701, doi:10.1029/2011GL049863.

Tett, S. F. B., M. J. Mineter, C. Cartis, D. J. Rowlands, and P. Liu (2013), Can top-of-atmosphere radiation measurements constrain climate predictions? Part I: Tuning, *J. Clim.*, *26*, 9348–9366.

Trenberth, K. E. (2011), Changes in precipitation with climate change, *Clim. Res.*, *47*, 123–138, doi:10.3354/cr00953.

Webb, M. J., F. H. Lambert, and J. M. Gregory (2012), Origins of differences in climate sensitivity, forcing and feedback in climate models, *Clim. Dyn.*, *40*, 677–707, doi:10.1007/s00382-012-1336-x.

Xie, S., H.-Y. Ma, J. S. Boyle, S. A. Klein, and Y. Zhang (2012), On the correspondence between short- and long-time-scale systematic errors in CAM4/CAM5 for the year of tropical convection, *J. Clim.*, *25*, 7937–7955, doi:10.1175/JCLI-D-12-00134.1.

Yamazaki, K., et al. (2013), Obtaining diverse behaviors in a climate model without the use of flux adjustments, *J. Geophys. Res. Atmos.*, *118*, 2781–2793, doi:10.1002/jgrd.50304.

Yokohata, T., J. D. Annan, J. C. Hargreaves, C. S. Jackson, M. Tobis, M. Webb, D. Sexton, and M. Collins (2012), Reliability of multi-model and structurally different single-model ensembles, *Clim. Dyn.*, *39*(3-4), 599–616, doi:10.1007/s00382-011-1203-1.

Yokohata, T., et al. (2013), Reliability and importance of structural diversity of climate model ensembles, *Clim. Dyn.*, doi:10.1007/s00382-013-1733-9.

Zamboni, L., J. D. Neelin, R. Jacob, M. Zhao, I. Held, and T. Moore (2014), *Simulation of Present-Climate Precipitation: Parameter Perturbations and Internal Variability With the GFDL Model, Paper Presented at American Geophysical Union Fall Meeting*, California, San Francisco.

Zhang, G. J., and N. A. McFarlane (1995), Sensitivity of climate simulations to the parameterization of cumulus convection in the Canadian climate centre general circulation model, *Atmos. Ocean*, *33*, 407–446.
Zhang, G. J., and H. Wang (2006), Toward mitigating the double ITCZ problem in NCAR CCSM3, *Geophys. Res. Lett.*, *33*, L06709, doi:10.1029/2005GL025229.
Zhang, G. J., et al. (2012), Regional assessment of the parameter-dependent performance of CAM4 in simulating tropical clouds, *Geophys. Res. Lett.*, *39*, L14708, doi:10.1029/2012GL052184.